Finite Element Methods for Quantum Electrodynamics Using a Helmholtz Decomposition of the Gauge Field

C. Ketelsen*, T. Manteuffel, S. McCormick and J. Ruge

Department of Applied Mathematics, Campus Box 526, University of Colorado at Boulder, Boulder, CO 80309-0526.

SUMMARY

The Dirac equation of quantum electrodynamics (QED) describes the interaction between electrons and photons. Large-scale numerical simulations of the theory require repeated solution of the two-dimensional Dirac equation, a system of two first-order partial differential equations coupled to a background U(1) gauge field. Traditional discretizations of this system are sparse and highly structured, but contain random complex entries introduced by the background field. For even mildly disordered gauge fields, the near kernel components of the system are highly oscillatory, rendering standard multilevel methods ineffective. We consider an alternate formulation of the governing equations obtained by a transformation of the continuum operator that decouples the system into separate scalar diffusion-like equations. We discretize the transformed system using least-squares finite elements and use adaptive smoothed aggregation multigrid (αSA) to solve the resulting linear system. We present numerical results and discuss implications of the transformed formulation in terms of the physical theory. Copyright © 2009 John Wiley & Sons, Ltd.

KEY WORDS: quantum electrodynamics, Dirac equation, lattice, finite elements, algebraic multigrid

1. Introduction

In the study of quantum electrodynamics (QED) and quantum chromodynamics (QCD), hybrid Monte Carlo simulations are used to numerically predict physical observables, such as particle mass and momentum, in accelerator experiments. The most computationally taxing portion of such simulations comes in the numerical solution of the discrete Dirac equation. Typical discretizations of the Dirac equation are large, sparse, and highly structured. Unfortunately, in the physically interesting parameter regime, the discrete operator is

---

*Correspondence to: Christian Ketelsen, Department of Applied Mathematics, Campus Box 526, University of Colorado at Boulder, Boulder, CO 80309-0526, U.S.A, E-mail: ketelsen@colorado.edu

extremely ill-conditioned and contains random complex entries, introduced by the background gauge field. Furthermore, as the particle mass, m, approaches realistic values, the traditional Krylov solvers become increasingly slow to converge, a phenomenon known as *critical slowing down*. Recently, algebraic multigrid (AMG) methods have proven to be effective preconditioners for the solution of the discrete Dirac equation, essentially eliminating critical slowing down [1] [2].

In addition to improving the iterative methods used to solve traditional discretizations of the Dirac equation, it is also important to consider new discretizations of the continuum operator that lend themselves to efficient solution by multilevel techniques. In a companion paper (see [3]), a discretization of a simplified 2-spin model of QED in two dimensions is developed using least-squares finite elements. We show here that the resulting discretization can be solved efficiently using an adaptive multilevel preconditioner. Additionally, we show that the resulting discrete system satisfies important physical properties of the continuum, including gauge invariance, chiral symmetry, and the absence of species doubling. The present paper expands on this method by first applying a transformation to the governing continuum equations and then discretizing the resulting system using least-squares finite elements. The discrete system is systematically developed and implications for the physical theory are discussed. When the discussion of the physical properties of the discretization reduces to the identical case as discussed in [3], we will refer the reader to the previous paper.

In the remainder of §1, we describe a simplified 2-spin model of QED in two dimensions, posed in the continuum. We introduce the concept of gauge invariance and propose a transformation of the continuum model that lends itself well to discretization using least-squares finite elements. In §2, the least-squares discretization of the transformed system is described along with several important properties of the resulting discrete system, including gauge invariance and the absence of species doubling [3]. In §3, we describe the use of adaptive smoothed aggregation multigrid (αSA) as a preconditioner for the solution process. Some concluding remarks are offered in §4.

1.1. Continuum Dirac Operator

The Dirac equation describes the behavior of spin-$\frac{1}{2}$ particles, or *fermions*. The governing equations can take on several different forms, depending on the specific gauge theory it describes. In particular, we are concerned with a 2-spin two-dimensional model of QED, which describes the interaction between electrons and photons. Another important configuration is the 4D Dirac equation of QCD, which describes the interaction between quarks and their force-carrying gluons. Though important in its own right for QED applications, the simplified model is often used as a starting point for testing discretizations and iterative solvers for the governing equations of full QCD.

In general, the Dirac equation appears as

$$\mathcal{D}\left(\mathcal{A}\right)\psi = f, \tag{1}$$

where $\mathcal{D}$ is the Dirac operator, $\mathcal{A}$ is the vector gauge field representing the force carriers, and f is some source term. In the simplified model of QED, (1) becomes:

$$\begin{bmatrix} mI & \nabla_x - i\nabla_y \\ \nabla_x + i\nabla_y & mI \end{bmatrix} \begin{bmatrix} \psi_R \\ \psi_L \end{bmatrix} = \begin{bmatrix} f_R \\ f_L \end{bmatrix}, \tag{2}$$

where $\nabla_x = (\partial_x - i\mathcal{A}_1)$ and $\nabla_y = (\partial_y - i\mathcal{A}_2)$ are the gauge covariant derivatives in the x- and y-directions, respectively . In this representation, m is the fermion mass, ∂_x and ∂_y are the usual partial derivatives, and $\mathcal{A}_\mu\left(x, y\right)$ is the μth component of the gauge field representing the photons. In QED, $\mathcal{A}_\mu\left(x, y\right) \in \mathbb{R}$, the set of real-valued scalars. The wavefunction $\psi = [\psi_R, \psi_L]^t$, describes the fermion, with two components, ψ_R and ψ_L, corresponding to fermion states that are *right-* and *left-handed*, respectively. *Handedness*, or *helicity*, is a description of the direction of a particle's angular momentum relative to its direction of motion. Similarly, the

source function, $f = [f_R, f_L]^t$, contains the right- and left-handed components of the source term [3], [4].

1.2. Model Problem

Let $\mathcal{R} = [0,1] \times [0,1]$ be the domain, $\mathcal{V}_\mathbb{R}$ be the space of real-valued, periodic functions that are uniformly bounded a.e. on $\mathcal{R}$, and $\mathcal{V}_\mathbb{C} \subset H^1(\mathcal{R})$ be the space of complex-valued, periodic, H^1 functions on $\mathcal{R}$ [5]. Let $\psi(x,y) = [\psi_R(x,y), \psi_L(x,y)]^t \in \mathcal{V}_\mathbb{C}^2$ be the fermion field with right- and left-handed components ψ_R and ψ_L, respectively. Assume that $\mathcal{A}(x,y) = [\mathcal{A}_1(x,y), \mathcal{A}_2(x,y)]^t \in \mathcal{V}_\mathbb{R}^2$. With periodic boundary conditions on ψ, the simplified model becomes

$$
\begin{bmatrix} mI & \nabla_x - i\nabla_y \\ \nabla_x + i\nabla_y & mI \end{bmatrix} \begin{bmatrix} \psi_R \\ \psi_L \end{bmatrix} = \begin{bmatrix} f_R \\ f_L \end{bmatrix} \text{ in } \mathcal{R}, \tag{3}
$$
$$
\psi(0,y) = \psi(1,y) \quad \forall y \in (0,1),
$$
$$
\psi(x,0) = \psi(x,1) \quad \forall x \in (0,1),
$$

To clarify notation, we emphasize that three different types of objects appear in this paper: continuum functions, finite element functions, and discrete vectors and operators. Continuum functions are denoted by scripted text, as in ψ, f, and $\mathcal{A}$. Operators in the continuum are represented in a similar scripted fashion, as in $\mathcal{D}$. Finite element functions are indicated with a superscript h, as in ψ^h, f^h, and A^h. Lastly, discrete vectors are denoted with an underbar, as in $\underline{\psi}$, $\underline{f}$, and $\underline{A}$, while discrete operators are denoted by bold-faced symbols, as in $\mathbb{D}$.

1.3. Gauge Covariance in the Continuum

A necessary property of any QED theory is that the *fermion propagator* - another name for $\mathcal{D}^{-1}$ - transforms *covariantly* under local gauge transformations, [6]. That is, suppose a local gauge transformation, $\Omega(x,y) \in U(1)$, is applied to each component of the fermion field ξ.

Then a modified propagator, $\widetilde{\mathcal{D}}^{-1}$, exists such that

$$\mathcal{D}^{-1} \begin{bmatrix} \Omega(x,y) & 0 \\ 0 & \Omega(x,y) \end{bmatrix} \xi = \begin{bmatrix} \Omega(x,y) & 0 \\ 0 & \Omega(x,y) \end{bmatrix} \widetilde{\mathcal{D}}^{-1} \xi.$$

Let $\Omega(x,y) = e^{i\omega(x,y)}$ for some real, periodic function ω. Suppose further that $\mathcal{D}$ is constructed using the gauge field $\mathcal{A}$. It is demonstrated in [3] that the correct modification of $\mathcal{D}^{-1}$ to allow gauge covariance is

$$\widetilde{\mathcal{D}}^{-1}(\mathcal{A}) = \mathcal{D}^{-1}(\mathcal{A} - \nabla\omega).$$

Thus,

$$\mathcal{D}^{-1}(\mathcal{A}) \begin{bmatrix} \Omega(x,y) & 0 \\ 0 & \Omega(x,y) \end{bmatrix} \xi = \begin{bmatrix} \Omega(x,y) & 0 \\ 0 & \Omega(x,y) \end{bmatrix} \mathcal{D}^{-1}(\mathcal{A} - \nabla\omega) \xi. \qquad (4)$$

A consequence of this is that, if we want to solve $\mathcal{D}(\mathcal{A})\psi = f$, then we are not restricted to working specifically with $\mathcal{D}(\mathcal{A})$. In fact, for *any* transformation of the form $\Omega(x,y) = e^{i\omega(x,y)} \in$ U(1) we have

$$\psi = \begin{bmatrix} \Omega(x,y) & 0 \\ 0 & \Omega(x,y) \end{bmatrix} \mathcal{D}^{-1}(\mathcal{A} - \nabla\omega) \begin{bmatrix} \Omega^*(x,y) & 0 \\ 0 & \Omega^*(x,y) \end{bmatrix} f. \qquad (5)$$

Then, if there exists some ω, such that $\mathcal{D}(\mathcal{A} - \nabla\omega)$ is easier to invert than $\mathcal{D}(\mathcal{A})$, we can solve the original problem for ψ by first applying the *inverse* transform to the source term f, inverting the transformed operator $\mathcal{D}(\mathcal{A} - \nabla\omega)$, and then applying the transformation to the

result.

1.4. Transformation

For simplicity, denote the off-diagonal block of (3) by $\mathcal{B}(\mathcal{A}) = \nabla_x - i\nabla_y = (\partial_x - i\mathcal{A}_1) - i(\partial_y - i\mathcal{A}_2)$. The matrix form of the Dirac equation then becomes

$$
\begin{bmatrix} mI & \mathcal{B} \\ -\mathcal{B}^* & mI \end{bmatrix} \begin{bmatrix} \psi_R \\ \psi_L \end{bmatrix} = \begin{bmatrix} f_R \\ f_L \end{bmatrix}. \tag{6}
$$

We begin by noting that operator $\mathcal{B}$ transforms covariantly under a transformation of the form e^z, where z is any complex-valued, periodic function. That is to say, if some component wavefunction ξ_R, which without loss of generality we take to be right-handed, is transformed according to $\xi_R \mapsto e^z \xi_R$, then it is possible to specify some modified operator $\widetilde{\mathcal{B}}$ such that

$$
\mathcal{B} e^z \xi_R = e^z \widetilde{\mathcal{B}} \xi_R.
$$

To see that $\mathcal{B}$ transforms covariantly under such a transformation, let $r(x, y)$ and $s(x, y)$ be real, periodic functions, and set $z = r + is$. Then

$$
\begin{aligned}
\mathcal{B}(\mathcal{A}) e^z \xi_R &= [(\partial_x - i\mathcal{A}_1) - i(\partial_y - i\mathcal{A}_2)] e^z \xi_R \\
&= e^z \{[\partial_x - i(\mathcal{A}_1 + r_y - s_x)] - i[\partial_y - i(\mathcal{A}_2 - r_x - s_y)]\} \xi_R \\
&= e^z \mathcal{B} \left(\mathcal{A} - \nabla^\perp r - \nabla s\right) \xi_R.
\end{aligned}
$$

Thus, the correct modification of $\mathcal{B}(\mathcal{A})$ corresponding to the transformation e^z is $\widetilde{\mathcal{B}} = \mathcal{B}\left(\mathcal{A} - \nabla^\perp r - \nabla s\right)$. Now, suppose that real, periodic functions u and v form a Helmholtz decomposition of the gauge field, according to

$$\mathcal{A} = \begin{bmatrix} \mathcal{A}_1 \\ \mathcal{A}_2 \end{bmatrix} = \nabla^{\perp} u + \nabla v + \begin{bmatrix} k_1 \\ k_2 \end{bmatrix}, \tag{7}$$

where k_1 and k_2 are constants. Setting $z = u + iv$, then

$$\mathcal{B}\left(\mathcal{A}\right) e^z \xi_R = e^z \mathcal{B}_k \xi_R, \tag{8}$$

where $\mathcal{B}_k := (\partial_x - ik_1) - i\,(\partial_y - ik_2)$. In addition, it is easy to verify that the adjoint operator, $\mathcal{B}^*$, transforms covariantly under a similar transformation. Specifically,

$$\mathcal{B}^*\left(\mathcal{A}\right) e^{-\bar{z}} \xi_R = e^{-\bar{z}} \mathcal{B}_k^* \xi_R. \tag{9}$$

We wish to use this property to separate the gauge field from the differential operators in $\mathcal{D}\left(\mathcal{A}\right)$. Define the following transformation matrix:

$$Q = \begin{bmatrix} e^{-\bar{z}} I & 0 \\ 0 & e^z I \end{bmatrix}. \tag{10}$$

Setting $\psi = Q\xi$, (6) yields

$$\begin{bmatrix} mI & \mathcal{B} \\ -\mathcal{B}^* & mI \end{bmatrix} \begin{bmatrix} e^{-\bar{z}} I & 0 \\ 0 & e^z I \end{bmatrix} \xi = f. \tag{11}$$

Using the covariance of $\mathcal{B}$, this becomes

$$
\begin{bmatrix}
me^{-\bar{z}}I & e^{z}\mathcal{B}_{k} \\
-e^{-\bar{z}}\mathcal{B}_{k}^{*} & me^{z}I
\end{bmatrix}
\xi \;=\; f.
\tag{12}
$$

Denote this transformed operator in (12) by $\hat{\mathcal{D}}(\mathcal{A})$. Note that we continue to express the dependence of $\hat{\mathcal{D}}$ on the gauge field, $\mathcal{A}$, because the gauge field still appears as part of the exponential terms. Then, if we have an efficient way of discretizing and solving the transformed system, (12), we can solve the original system, (6), by first solving (12) and then setting $\psi = Q\xi$. Thus, a solution process for the continuum problem is given in Algorithm 1.

ALGORITHM 1: Continuum Dirac Solve

- *Input:* Gauge field $\mathcal{A}$, source term f.
- *Output:* Wavefunction ψ.

1. Solve $\hat{\mathcal{D}}(\mathcal{A})\xi = f$.
2. Set $\psi = Q\xi$.

Note that we must be careful with the boundary conditions prescribed to the auxiliary function ξ. To ensure that ψ is periodic on $\mathcal{R}$, we require that $Q\xi$ be periodic on $\mathcal{R}$. To discretize the continuum equation in Step 1 of Algorithm 1, we use least-squares finite elements [7], [8].

In addition to providing a potential solution method for (6), this transformation also gives insight into the spectrum of the continuum operator. First, note that, from the form of (6), the Dirac operator can be written as the sum of Hermitian and anti-Hermitian operators:

$$
\begin{bmatrix}
mI & \mathcal{B} \\
-\mathcal{B}^{*} & mI
\end{bmatrix}
\;=\;
\begin{bmatrix}
mI & 0 \\
0 & mI
\end{bmatrix}
+
\begin{bmatrix}
0 & \mathcal{B} \\
-\mathcal{B}^{*} & 0
\end{bmatrix}.
\tag{13}
$$

Thus, the spectrum of $\mathcal{D}$ is a vertical line in the complex plane:

$$\Sigma\left(\mathcal{D}\right) \quad = \quad m + is_j, \tag{14}$$

where $s_j \in \mathbb{R}$, $j = 1, 2, \ldots$ Furthermore, note that $\mathcal{D}$ has a purely real eigenvalue if and only if k_1 and k_2 are integer multiples of 2π. To see this, consider the transformed operator $\mathcal{B}_k$, with the non-constant portion of the gauge field removed. Let $\phi = e^{i(k_1 x + k_2 y)}$. Then,

$$
\begin{aligned}
\mathcal{B}_k \phi \quad &= \quad \left[\left(\partial_x - ik_1\right) - i\left(\partial_y - ik_2\right)\right] e^{i(k_1 x + k_2 y)}, \\
&= \quad \left[\left(ik_1 - ik_1\right) - i\left(ik_2 - ik_2\right)\right] e^{i(k_1 x + k_2 y)}, \\
&= \quad 0.
\end{aligned}
$$

But, recall that operator $\mathcal{B}_k$ acts on complex-valued periodic functions and that

$$e^{i(k_1 x + k_2 y)} \quad = \quad \left[\cos\left(k_1 x\right) + i\sin\left(k_1 x\right)\right]\left[\cos\left(k_2 y\right) + i\sin\left(k_2 y\right)\right].$$

Then, $\phi = e^{i(k_1 x + k_2 y)}$ is periodic on $\mathcal{R}$ only if $k_1 = 2\pi l_1$ and $k_2 = 2\pi l_2$ for some $l_1, l_2 \in \mathbb{Z}$. Thus, it is easy to see from (8) that operator $\mathcal{B}\left(\mathcal{A}\right)$ is singular, with nullspace vector $\phi = e^{z + i(k_1 x + k_2 y)}$, only if k_1 and k_2 are integer multiples of 2π. Similarly, from (9), it is clear that, under these conditions on $\underline{k}$, $\mathcal{B}^*\left(\mathcal{A}\right)$ is singular with nullspace vector $\phi = e^{-\bar{z} + i(k_1 x + k_2 y)}$. Then, from (13), we see that if the constant portions of the gauge field are integer multiples of 2π, then $\mathcal{D}$ has two eigenvectors, ϕ_+ and ϕ_-, associated with purely real eigenvalue m, where

$$\phi_+ = \begin{bmatrix} e^{-\bar{z}+i(k_1 x + k_2 y)} \\ e^{z+i(k_1 x + k_2 y)} \end{bmatrix},$$

$$\phi_- = \begin{bmatrix} e^{-\bar{z}+i(k_1 x + k_2 y)} \\ -e^{z+i(k_1 x + k_2 y)} \end{bmatrix}.$$

2. Discrete Dirac Operator

In numerical simulations of QED, it is necessary to compute many solutions of the discrete Dirac equation for varying gauge fields and source vectors. In traditional lattice formulations, the continuum domain, $\mathcal{R}$, is replaced by an $n \times n$ regular, periodic lattice. The continuum wavefunction, ψ, and source, f, are replaced by discrete analogues, $\underline{\psi}$ and $\underline{f}$, with values specified only at the lattice *sites*. The continuum gauge field, $\mathcal{A}$, is represented by the discrete field $\underline{A} = [\underline{A}_1, \underline{A}_2]^t$, with information specified on each of the lattice *links*. The components of the gauge field, $\underline{A}_1$ and $\underline{A}_2$, represent values on the horizontal and vertical lattice links, respectively. A discrete solution process of the 2D model problem then takes the source, $\underline{f}$, specified at the lattice sites, and gauge field, $\underline{A}$, specified at the lattice links, and returns the discrete fermion field $\underline{\psi}$, with values again specified at the lattice sites. The discrete solution can be written as

$$\underline{\psi} = [\mathbb{D}(\underline{A})]^{-1} \underline{f},$$

where $[\mathbb{D}(\underline{A})]^{-1}$ is some discrete representation of the solution process.

For completeness, let $\mathcal{N}_{\mathbb{C}}$ be the space of discrete, periodic, complex-valued vectors, with values associated with the sites on the lattice. Let $\mathcal{N}_{\mathbb{R}} \subset \mathcal{N}_{\mathbb{C}}$ be the space of discrete real-valued vectors, with values associated with the lattice sites. Then, the discrete fermion field is given by $\underline{\psi} = [\underline{\psi}_R, \underline{\psi}_L]^t \in \mathcal{N}_{\mathbb{C}}^2$, which specifies complex values of both the right- and left-

handed components of the fermion field at each lattice site. Similarly, the source term, f, becomes $\underline{f} = [\underline{f}_R, \underline{f}_L]^t \in \mathcal{N}_{\mathbb{C}}^2$. Let $\mathcal{E}_{\mathbb{R}}$ be the space of discrete real-valued vectors, with values associated with the lattice links. Then $\underline{A} = [\underline{A}_1, \underline{A}_2]^t \in \mathcal{E}_{\mathbb{R}}$.

2.1. Preliminary Considerations

To formulate the discrete Dirac equation in terms of a finite-element process, we must associate the discrete objects, $\underline{\psi}$, $\underline{A}$, and $\underline{f}$, with corresponding finite-element functions. In analogy to the nodal setting, each elementary square on the lattice is represented by a quadrilateral finite element. Recall that $\mathcal{N}_{\mathbb{C}}$ is the space of discrete complex-valued vectors, with values associated with the lattice sites. We equate any discrete vector $\underline{w} = \left[\underline{w}_R, \underline{w}_L\right]^t \in (\mathcal{N}_{\mathbb{C}})^2$ with the piecewise bilinear function $w^h = \left[w_R^h, w_L^h\right]^t \in \left(\mathcal{V}_{\mathbb{C}}^h\right)^2$, where $\mathcal{V}_{\mathbb{C}}^h = \mathrm{span}\{\phi_j\}_{j=1}^{n^2}$ is the space of periodic piecewise bilinear finite element functions over the complex numbers. Here, ϕ_j is the standard nodal basis function associated with lattice site x_j. Then, naturally,

$$
\begin{aligned}
w_R^h &= \sum_{j=1}^{n^2} \underline{w}_{Rj}\phi_j, \\
w_L^h &= \sum_{j=1}^{n^2} \underline{w}_{Lj}\phi_j.
\end{aligned}
$$

We wish to represent the discrete gauge field, $\underline{A}$, in the continuum using a finite element function. Recall that $\underline{A} = [\underline{A}_1, \underline{A}_2]^t$ belongs to $\mathcal{E}_{\mathbb{R}}$, the space of discrete real-valued vectors, with values associated with the lattice links. Gauge data, $\underline{A}_1$ and $\underline{A}_2$, define values on the horizontal and vertical lattice links, respectively. We associate any $\underline{A} \in \mathcal{E}_{\mathbb{R}}$ with $A^h = \left[A_1^h, A_2^h\right]^t \in \mathcal{W}_{\mathbb{R}}^h$, where A^h is chosen to exactly interpolate the discrete gauge data on the centers of lattice links. To define A^h and $\mathcal{W}_{\mathbb{R}}^h$ precisely we first consider a Helmholtz decomposition of the discrete gauge field:

$$
\underline{A} \;=\; \begin{bmatrix} \underline{A}_1 \\[2mm] \underline{A}_2 \end{bmatrix} \;=\; \begin{bmatrix} \mathbb{C}_1 & \mathbb{G}_1 \\[2mm] \mathbb{C}_2 & \mathbb{G}_2 \end{bmatrix} \begin{bmatrix} \underline{u} \\[2mm] \underline{v} \end{bmatrix} + \begin{bmatrix} \underline{k}_1 \\[2mm] \underline{k}_2 \end{bmatrix} \tag{15}
$$

where $\mathbb{C} = [\mathbb{C}_1^t \;\; \mathbb{C}_2^t]^t$ and $\mathbb{G} = [\mathbb{G}_1^t \;\; \mathbb{G}_2^t]^t$ are discrete representations of the curl and gradient operators, respectively. The specific forms of $\mathbb{C}$ and $\mathbb{G}$ are given below. Vectors $\underline{v}$ and $\underline{u}$ are real-valued and are associated with the sites of the standard lattice and the cell-centered lattice, respectively. Then $\underline{u}, \underline{v} \in \mathcal{N}_{\mathbb{R}}$. Note that each row in (15) corresponds to gauge data on a link on the standard lattice, with the first block row corresponding to the horizontal links and the second block row corresponding to the vertical links. The rows of the matrix in (15), denoted alternatively by $[\mathbb{C} \;\; \mathbb{G}]$, are defined by the relationship between the individual lattice links and their contributions from $\underline{u}$ and $\underline{v}$ values on adjoining lattice sites. As such, the rows of matrices $\mathbb{G}$ and $\mathbb{C}$ are defined by the appropriate centered differences that map values of $\underline{v}$ and $\underline{u}$ at sites on the standard and cell-centered lattice, respectively, to values on the links of the standard lattice. The stencils for constituent matrices of $\mathbb{C}$ and $\mathbb{G}$ are as follows:

$$
\mathbb{C}_1 \;=\; \frac{1}{h} \begin{bmatrix} 0 & -1 & 0 \\ 0 & 1 & 0 \\ 0 & 0 & 0 \end{bmatrix}, \tag{16}
$$

$$
\mathbb{C}_2 \;=\; \frac{1}{h} \begin{bmatrix} 0 & 0 & 0 \\ -1 & 1 & 0 \\ 0 & 0 & 0 \end{bmatrix}, \tag{17}
$$

$$\mathbb{G}_1 \;=\; \frac{1}{h} \begin{bmatrix} 0 & 0 & 0 \\ -1 & 1 & 0 \\ 0 & 0 & 0 \end{bmatrix}, \tag{18}$$

$$\mathbb{G}_2 \;=\; \frac{1}{h} \begin{bmatrix} 0 & 0 & 0 \\ 0 & 1 & 0 \\ 0 & -1 & 0 \end{bmatrix}. \tag{19}$$

Inspection of these stencils shows that constant vectors are in the nullspace of both $\mathbb{C}$ and $\mathbb{G}$, so the decomposition defined in (15) is not unique; any $\underline{u}$ and $\underline{\hat{u}}$, or any $\underline{v}$ and $\underline{\hat{v}}$, that differ by only a constant produce the same $\underline{A}$. To remedy this, we require that the entries of $\underline{u}$ and $\underline{v}$ individually sum to zero. That is, we require that

$$\sum_{jk} \underline{u}_{jk} \;=\; \sum_{jk} \underline{v}_{jk} \;=\; 0.$$

Under these conditions, the decomposition defined in (15) is unique.

The development of the decomposition in (15) suggests a method of computing $\underline{v}$ and $\underline{u}$ for any gauge field, $\underline{A}$. Specifically, $\underline{u}$ is the orthogonal projection of $\underline{A}$ onto the space of vectors in Range $(\mathbb{C})$ whose entries sum to zero. Likewise, $\underline{v}$ is the orthogonal projection of $\underline{A}$ onto the space of vectors in Range $(\mathbb{G})$ whose entries sum to zero. Thus, $\underline{u}$ and $\underline{v}$ are the solutions to the following sets of normal equations:

$$\hat{\mathbb{C}}^t \hat{\mathbb{C}} \underline{u} \;=\; \hat{\mathbb{C}}^t \underline{A}, \tag{20}$$

$$\hat{\mathbb{G}}^t \hat{\mathbb{G}} \underline{v} \;=\; \hat{\mathbb{G}}^t \underline{A}, \tag{21}$$

where $\hat{\mathbb{C}}$ and $\hat{\mathbb{G}}$ are nonsingular versions of $\mathbb{C}$ and $\mathbb{G}$ modified to enforce the condition that the

entries of $\underline{u}$ and $\underline{v}$ sum to zero. The matrices on the left-hand side of (20) and (21) are similar to constant coefficient periodic Poisson operators discretized via finite differences. Thus, they can easily be inverted using standard methods. Finally, constants k_1 and k_2 are found by computing

$$\left[\begin{array}{c} \underline{k_1} \\ \underline{k_2} \end{array} \right] \quad = \quad \underline{A} - \mathbb{C}\underline{u} - \mathbb{G}\underline{v}. \tag{22}$$

The development of the Helmholtz decomposition of the discrete gauge field leads us to a convenient representation of the discrete gauge data by a finite element function, A^h. Note that the action of $\mathbb{G}$ and $\mathbb{C}$ on discrete vectors can be interpreted as the application of the gradient and curl operators to bilinear finite element functions defined on the standard and cell-centered lattice, respectively. Then, A^h can be defined in terms of a continuum Helmholtz decomposition involving bilinear finite element functions v^h and u^h defined on the standard and cell-centered lattice, respectively, whose entries at lattice sites correspond exactly with the discrete values of $\underline{v}$ and $\underline{u}$. This decomposition is

$$A^h \quad = \quad \nabla^\perp u^h + \nabla v^h + \underline{k}. \tag{23}$$

The definition of v^h as a bilinear finite element function on the standard lattice implies that the gradient portion of the gauge field, ∇v^h, belongs to $\mathcal{W}_v^h$, the Nédélec space over the real numbers associated with the standard lattice. Similarly, the definition of u^h as a bilinear finite element function on the cell-centered lattice implies that the curl portion of the gauge filed, $\nabla^\perp u^h$, belongs to $\mathcal{W}_u^h$, the Raviart-Thomas space over the real numbers associated with a cell-centered lattice. Illustrations of typical basis functions for $\mathcal{W}_u^h$ and $\mathcal{W}_v^h$ can be found in Figures 1 and 2. Noting that constant vector $\underline{k}$ is represented in both of these spaces, define $\mathcal{W}_\mathbb{R}^h = \mathcal{W}_u^h \oplus \mathcal{W}_v^h$. This choice of spaces naturally ensures that the curl and gradient portions
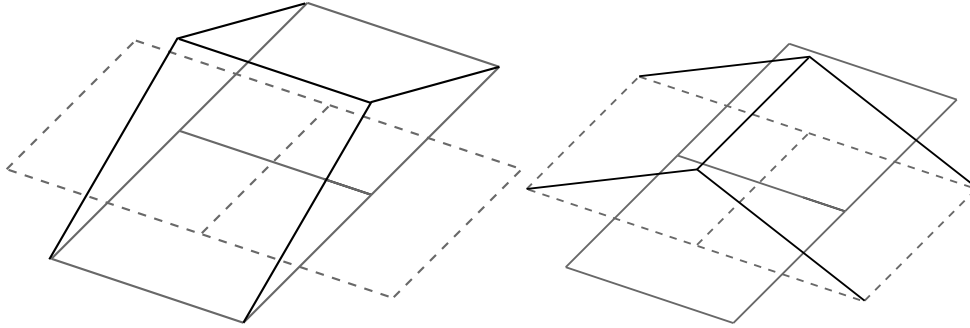
of the gauge field are orthogonal.

Figure 1: Nédélec element (left) and Raviart-Thomas element (right) associated with a horizontal lattice. The solid grid lines represent the standard lattice, and the dashed represent the cell-centered lattice
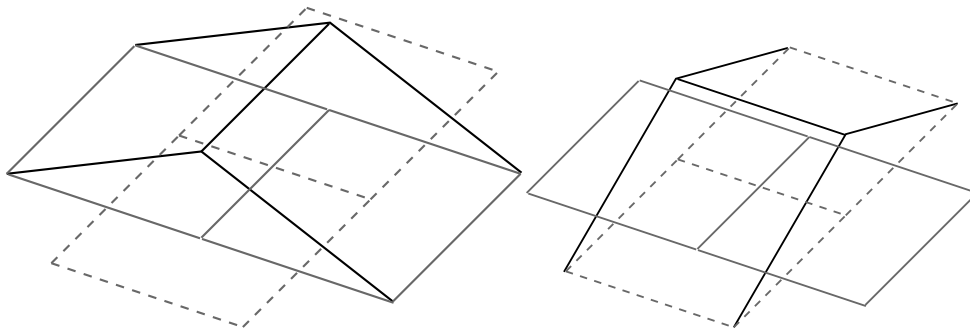

Figure 2: Nédélec element (left) and Raviart-Thomas element (right) associated with a vertical lattice. The solid grid lines represent the standard lattice, and the dashed represent the cell-centered lattice

2.2. Least-Squares Discretization

We begin by formulating the solution to (12), appearing in Step 1 of Algorithm 1, in terms of a minimization principle.

$$\xi \quad = \quad \arg\min_{\varphi \in \mathcal{V}_{\mathbb{C}}^2} \|\hat{\mathcal{D}}\varphi - f\|_0^2, \tag{24}$$

where $\mathcal{V}_{\mathbb{c}}$ is the space of continuous, periodic, complex-valued, H^1 functions defined previously. Minimization principle (24) is equivalent to the following weak form:

$$\text{Find } \xi \in \mathcal{V}_{\mathbb{c}}^2 \text{ s.t. } \left\langle \hat{\mathcal{D}}\xi, \hat{\mathcal{D}}w \right\rangle = \left\langle f, \hat{\mathcal{D}}w \right\rangle \quad \forall w \in \mathcal{V}_{\mathbb{c}}^2, \tag{25}$$

where $\langle \, \cdot \, , \, \cdot \, \rangle$ is the usual L^2 inner product. If ξ is sufficiently smooth, then (25) is formally equivalent to

$$\text{Find } \xi \in \mathcal{V}_{\mathbb{c}}^2 \text{ s.t. } \left\langle \hat{\mathcal{D}}^*\hat{\mathcal{D}}\xi, w \right\rangle = \left\langle \hat{\mathcal{D}}^* f, w \right\rangle \quad \forall w \in \mathcal{V}_{\mathbb{c}}^2. \tag{26}$$

Thus, we can think of the least-squares formulation of the problem as being approximately equivalent to solving the continuum normal equations, $\hat{\mathcal{D}}^*\hat{\mathcal{D}}\xi = \hat{\mathcal{D}}^* f$, by the Ritz-Galerkin method. Examining the *formal normal* operator, $\hat{\mathcal{D}}^*\hat{\mathcal{D}}$, can often give insight into the potential success of the least-squares formulation:

$$\hat{\mathcal{D}}^*\hat{\mathcal{D}} = \begin{bmatrix} me^{-z}I & -\mathcal{B}_k e^{-z} \\ \mathcal{B}_k^* e^{\bar{z}} & me^{\bar{z}}I \end{bmatrix} \begin{bmatrix} me^{-\bar{z}}I & e^z \mathcal{B}_k \\ -e^{-\bar{z}}\mathcal{B}_k^* & me^z I \end{bmatrix} \tag{27}$$

$$= \begin{bmatrix} m^2 e^{-2u}I + \mathcal{B}_k^* e^{-2u}\mathcal{B}_k & 0 \\ 0 & m^2 e^{2u}I + \mathcal{B}_k e^{2u}\mathcal{B}_k^* \end{bmatrix}. \tag{28}$$

Notice that v, which is associated with the gradient portion of the gauge field, vanishes from the formal normal. Moreover, this formal normal is block diagonal, with each diagonal block containing a zeroth-order term and a second-order term resembling a diffusion operator with variable coefficients. This is promising because algebraic multigrid methods have proved effective at solving these types of problems [7], [8].

The least-squares solution is obtained by restricting the minimization problem in (24) and,

thus, the weak form in (25), to a finite-dimensional space, $\mathcal{V}_{\mathbb{C}}^h \subset \mathcal{V}_{\mathbb{C}}$. That is, our solution must satisfy the following weak form:

$$\text{Find } \xi^h \in \left(\mathcal{V}_{\mathbb{C}}^h\right)^2 \text{ s.t. } \left\langle \hat{\mathcal{D}}\xi^h, \hat{\mathcal{D}}w^h \right\rangle \quad = \quad \left\langle f^h, \hat{\mathcal{D}}w^h \right\rangle \quad \forall w^h \in \left(\mathcal{V}_{\mathbb{C}}^h\right)^2. \tag{29}$$

Step 2 of Algorithm 1 requires that we set $\psi = Q\xi$. We can formulate this process in terms of a weak form as well:

$$\text{Find } \psi^h \in \left(\mathcal{V}_{\mathbb{C}}^h\right)^2 \text{ s.t. } \left\langle \psi^h, w^h \right\rangle \quad = \quad \left\langle Q\xi^h, w^h \right\rangle \quad \forall w^h \in \left(\mathcal{V}_{\mathbb{C}}^h\right)^2. \tag{30}$$

The least-squares formulation of Algorithm 1 can now be implemented via the following algorithm:

ALGORITHM 2: Least-Squares Dirac Solve

- *Input:* Gauge field $\underline{A}$, source term $\underline{f}$.
- *Output:* Wavefunction $\underline{\psi}$.

1. Compute $\underline{u}$ and $\underline{v}$ such that $\underline{A} = \mathbb{C}\underline{u} + \mathbb{G}\underline{v} + \underline{k}$.
2. Map $\underline{u} \mapsto u^h$ and $\underline{v} \mapsto v^h$.
3. Map $\underline{f} \mapsto f^h \in \left(\mathcal{V}_{\mathbb{C}}^h\right)^2$.
4. Find $\xi^h \in \left(\mathcal{V}_{\mathbb{C}}^h\right)^2$ s.t. $\left\langle \hat{\mathcal{D}}\xi^h, \hat{\mathcal{D}}w^h \right\rangle = \left\langle f^h, \hat{\mathcal{D}}w^h \right\rangle \quad \forall w^h \in \left(\mathcal{V}_{\mathbb{C}}^h\right)^2,$

5. Find $\psi^h \in \left(\mathcal{V}_{\mathbb{C}}^h\right)^2$ s.t. $\left\langle \psi^h, w^h \right\rangle = \left\langle Q\xi^h, w^h \right\rangle \quad \forall w^h \in \left(\mathcal{V}_{\mathbb{C}}^h\right)^2,$

6. Map $\psi^h \mapsto \underline{\psi} \in \left(\mathcal{N}_{\mathbb{C}}\right)^2.$

Using the nodal basis for $\mathcal{V}_{\mathbb{C}}^h$, we can form the following matrix equation for solving the weak form in Step 4 of Algorithm 2:

$$\mathbb{L}\underline{\xi} = \mathbb{K}\underline{f}, \tag{31}$$

where $\underline{\xi}$ and $\underline{f}$ are the coefficients in the expansions of ξ^h and f^h, respectively. Note that since the discrete values of $\underline{\xi}$ and $\underline{f}$ naturally coincide with the expansion coefficients of ξ^h and f^h, respectively, we choose to represent them using the same notation. Matrices $\mathbb{L}$ and $\mathbb{K}$ are given according to

$$\mathbb{L} \quad := \quad \begin{bmatrix} \mathbb{L}_{11} & 0 \\ 0 & \mathbb{L}_{22} \end{bmatrix}, \tag{32}$$

$$\mathbb{L}_{11} \quad := \quad m^2\mathbb{M}^- + \mathbb{L}_{xx}^- + \mathbb{L}_{yy}^- + i(\mathbb{L}_{xy}^- - \mathbb{L}_{yx}^-), \tag{33}$$

$$\mathbb{L}_{22} \quad := \quad m^2\mathbb{M}^+ + \mathbb{L}_{xx}^+ + \mathbb{L}_{yy}^+ + i(\mathbb{L}_{xy}^+ - \mathbb{L}_{yx}^+), \tag{34}$$

$$\mathbb{K} \quad = \quad \begin{bmatrix} m\mathbb{N}^+ & \mathbb{B}_x^+ - i\mathbb{B}_y^+ \\ \mathbb{B}_x^- + i\mathbb{B}_y^- & m\mathbb{N}^- \end{bmatrix}, \tag{35}$$

where

$$
\begin{aligned}
(\mathbb{L}_{xx}^{\pm})_{j,k} &= \left\langle e^{\pm u} \left(\partial_x - ik_1\right) \phi_k, e^{\pm u} \left(\partial_x - ik_1\right) \phi_j \right\rangle, \\[4pt]
(\mathbb{L}_{yy}^{\pm})_{j,k} &= \left\langle e^{\pm u} \left(\partial_y - ik_2\right) \phi_k, e^{\pm u} \left(\partial_y - ik_2\right) \phi_j \right\rangle, \\[4pt]
(\mathbb{L}_{xy}^{\pm})_{j,k} &= \left\langle e^{\pm u} \left(\partial_x - ik_1\right) \phi_k, e^{\pm u} \left(\partial_y - ik_2\right) \phi_j \right\rangle, \\[4pt]
(\mathbb{L}_{yx}^{\pm})_{j,k} &= \left\langle e^{\pm u} \left(\partial_y - ik_2\right) \phi_k, e^{\pm u} \left(\partial_x - ik_1\right) \phi_j \right\rangle, \\[4pt]
(\mathbb{B}_{x}^{\pm})_{j,k} &= \left\langle \phi_k, e^{\pm u + iv} \left(\partial_x - ik_1\right) \phi_j \right\rangle, \\[4pt]
(\mathbb{B}_{y}^{\pm})_{j,k} &= \left\langle \phi_k, e^{\pm u + iv} \left(\partial_y - ik_2\right) \phi_j \right\rangle, \\[4pt]
(\mathbb{M}^{\pm})_{j,k} &= \left\langle e^{\pm u} \phi_k, e^{\pm u} \phi_j \right\rangle, \\[4pt]
(\mathbb{N}^{\pm})_{j,k} &= \left\langle \phi_k, e^{\pm u + iv} \phi_j \right\rangle.
\end{aligned}
\tag{36}
$$

Thus, Step 4 of Algorithm 2 can then be replaced by

$$
\xi = \mathbb{L}^{-1} \mathbb{K} \underline{f}.
\tag{37}
$$

A similar linear system can be developed to replace the weak form in Step 5 of Algorithm 2:

$$
\mathbb{P} \underline{\psi} = \mathbb{Q} \underline{\xi}.
\tag{38}
$$

where

$$
\mathbb{P} =
\begin{bmatrix}
\mathbb{P}_0 & 0 \\
0 & \mathbb{P}_0
\end{bmatrix}, \qquad
\mathbb{Q} =
\begin{bmatrix}
\mathbb{Q}^- & 0 \\
0 & \mathbb{Q}^+
\end{bmatrix},
\tag{39}
$$

and

$$(\mathbb{P}_0)_{j,k} = <\phi_k, \phi_j>, \quad (\mathbb{Q}^{\pm})_{j,k} = <e^{\pm u+iv}\phi_k, \phi_j>. \tag{40}$$

Again, since the expansion coefficients of ψ^h correspond to the discrete values in $\underline{\psi}$, we can replace both Step 5 and Step 6 of Algorithm 2 by

$$\underline{\psi} = \mathbb{P}^{-1}\mathbb{Q}\underline{\xi}. \tag{41}$$

It is useful to note that $\mathbb{L}$ and $\mathbb{P}$ do not depend on v in any way. They are defined solely in terms of the curl component of the gauge field.

Finally, these associations allow us to write a discrete solution process, equivalent to Algorithm 2, solely in terms of the discrete variables:

ALGORITHM 3: Discrete Dirac Solve

- *Input:* Gauge field $\underline{A}$, source term $\underline{f}$.
- *Output:* Wavefunction $\underline{\psi}$.

1. Compute $\underline{u}$ and $\underline{v}$ such that $\underline{A} = \mathbb{C}\underline{u} + \mathbb{G}\underline{v} + \underline{k}$.
2. Compute $\underline{\xi} = \mathbb{L}^{-1}\mathbb{K}\underline{f}$.
3. Compute $\underline{\psi} = \mathbb{P}^{-1}\mathbb{Q}\underline{\xi}$.

2.3. Gauge Covariance of the Discrete Solution Process

A little reflection on the property of gauge covariance of the fermion propagator in the continuum leads us to a test for covariance of the discrete solution process. Suppose that, in the continuum, we are given related Dirac equations:

$$\mathcal{D}\left(\mathcal{A}\right)\psi = f,$$

$$\mathcal{D}\left(\mathcal{A} - \nabla\theta\right)\widetilde{\psi} = \left[\begin{array}{cc} \Omega^*\left(x,y\right) & 0 \\ 0 & \Omega^*\left(x,y\right) \end{array}\right]f,$$

where $\Omega\left(x,y\right) = e^{i\theta(x,y)}$ for some θ. Then, by the principle of gauge covariance, we have

$$\psi = \left[\begin{array}{cc} \Omega\left(x,y\right) & 0 \\ 0 & \Omega\left(x,y\right) \end{array}\right]\widetilde{\psi}.$$

Transferring these facts to the discrete lattice, we let $\underline{\theta}$ be the vector of values of $\theta\left(x,y\right)$ on the lattice sites and define discrete gauge transformation $\underline{\Omega}_{\underline{\theta}}$ by a diagonal matrix such that

$$\left(\underline{\Omega}_{\underline{\theta}}\right)_{kk} = e^{i\theta_k}.$$

The adjoint of this transformation, $\underline{\Omega}^*_{\underline{\theta}}$ is the diagonal matrix such that

$$\left(\underline{\Omega}^*_{\underline{\theta}}\right)_{kk} = e^{-i\theta_k}.$$

Finally, define the respective transformation matrix and its adjoint, which operate on two-component wavefunctions by

$$\mathbb{T}_{\underline{\theta}} = \left[\begin{array}{cc} \underline{\Omega}_{\underline{\theta}} & 0 \\ 0 & \underline{\Omega}_{\underline{\theta}} \end{array}\right] \quad \mathbb{T}^*_{\underline{\theta}} = \left[\begin{array}{cc} \underline{\Omega}^*_{\underline{\theta}} & 0 \\ 0 & \underline{\Omega}^*_{\underline{\theta}} \end{array}\right].$$

Suppose now that we are given two sets of gauge data, $\underline{A}$ and $\underline{\widetilde{A}}$, and two sets of source data, $\underline{f}$ and $\underline{\widetilde{f}}$, related according to

$$\underline{\widetilde{A}} \;=\; \underline{A} - \mathbb{G}\theta, \tag{42}$$

$$\underline{\widetilde{f}} \;=\; \mathbb{T}_{\underline{\theta}}^{*}\,\underline{f}. \tag{43}$$

Then, given these two sets of inputs, Algorithm 3 should yield solution vectors, $\underline{\psi}$ and $\underline{\widetilde{\psi}}$, such that

$$\underline{\psi} \;=\; \mathbb{T}_{\underline{\theta}}\,\underline{\widetilde{\psi}}.$$

Surely, if the solution of the auxiliary system appearing in Step 2 of Algorithm 3 is not gauge covariant, then Algorithm 3 as a whole will not be either. Thus, we first ask whether, given the above data, Steps 1-2 return vectors $\underline{\xi}$ and $\underline{\widetilde{\xi}}$ that satisfy

$$\underline{\xi} \;=\; \mathbb{T}_{\underline{\theta}}\,\underline{\widetilde{\xi}}.$$

Upon closer examination of the derivation of the algorithm, we realize that this cannot be true. The problem arises in the weak form appearing in Step 4 of Algorithm 2. The weak form for the modified data appears as

$$\text{Find } \widetilde{\xi}^{h} \in \left(\mathcal{V}_{\mathbb{C}}^{h}\right)^{2} \text{ s.t. } \left\langle \hat{\mathcal{D}}\widetilde{\xi}^{h}, \hat{\mathcal{D}}w^{h} \right\rangle \;=\; \left\langle \widetilde{f}^{h}, \hat{\mathcal{D}}w^{h} \right\rangle \quad \forall w^{h} \in \left(\mathcal{V}_{\mathbb{C}}^{h}\right)^{2},$$

where $\widetilde{f}^{h}$ is the projection of $\mathbb{T}_{\underline{\theta}}^{*}\,\underline{f}$ into the space of piecewise bilinears. The problem arises in the inner product on the right hand side of this equality. Assuming that the Helmholtz decomposition of the modified gauge field is given by $\widetilde{\mathcal{A}} = \nabla^{\perp}u^{h} + \nabla\left(v^{h} - \theta^{h}\right) + k^{h}$, we can

rewrite this inner product as

$$\left\langle \left[\begin{array}{cc} e^{-i(v-\theta)} & 0 \\ 0 & e^{-i(v-\theta)} \end{array} \right] \widetilde{f}^h, \left[\begin{array}{cc} me^{-u}I & e^u\mathcal{B}_k \\ -e^{-u}\mathcal{B}_k^* & me^uI \end{array} \right] w^h \right\rangle.$$

To achieve covariance, we need the exponential term embedded in $\widetilde{f}^h$, as shown in (43), to cancel with the $e^{i\theta}$ term in the inner product. Unfortunately, the fact that the exponential in $\widetilde{f}^h$ has been projected into a bilinear space, and that the inner product is traditionally evaluated numerically using quadrature points not located at lattice sites, defeats exact cancelation. A similar problem arises in the weak form used to transform ξ^h into ψ^h.

Fortunately, this difficulty occurs only in the imaginary part of the transformation. We can thus remedy this problem, and in turn restore gauge covariance, by treating the imaginary part of the transformation in the lattice setting, and the real part in the finite-element setting.

Recall from (5) that, for any transformation $\Omega(x,y) = e^{i\omega(x,y)}$, we are free to solve $\mathcal{D}(\mathcal{A})\psi = f$ for ψ by solving the modified problem

$$\mathcal{D}(\mathcal{A} - \nabla\omega)\widetilde{\psi} = \left[\begin{array}{cc} \Omega^*(x,y) & 0 \\ 0 & \Omega^*(x,y) \end{array} \right] f \tag{44}$$

and then setting

$$\psi = \left[\begin{array}{cc} \Omega(x,y) & 0 \\ 0 & \Omega(x,y) \end{array} \right] \widetilde{\psi}. \tag{45}$$

Then, if $\mathcal{A}$ has the Helmholtz decomposition given in (7), choosing $\omega = v$ eliminates the gradient and constant portions of the gauge field, and, thus, all imaginary parts from the transformation. That is, the intermediate problem becomes

$$\mathcal{D}\left(\nabla^{\perp}u\right)\widetilde{\psi} \;=\; \left[\begin{array}{cc} \Omega^{*}\left(x,y\right) & 0 \\ 0 & \Omega^{*}\left(x,y\right) \end{array}\right] f. \tag{46}$$

After solving for the approximation to $\widetilde{\psi}$ using the least-squares formulation, we obtain the approximation to ψ on the lattice by setting

$$\underline{\psi} \;=\; \mathbb{T}_{\underline{v}}\,\widetilde{\underline{\psi}}. \tag{47}$$

Note that the only changes made in the finite-element solution process is that $\mathbb{K}$ and $\mathbb{Q}$ are constructed with the gradient portion of the gauge field set to 0. We can now formulate a discrete Dirac solver that exhibits gauge covariance.

ALGORITHM 4: Gauge Covariant Discrete Dirac Solve

- *Input:* Gauge field $\underline{A}$, source term $\underline{f}$.
- *Output:* Wavefunction $\underline{\psi}$.

1. Compute $\underline{u}$ and $\underline{v}$ such that $\underline{A} = \mathbb{C}\underline{u} + \mathbb{G}\underline{v} + \underline{k}$.
2. Set $\underline{g} = \mathbb{T}_{\underline{v}}^{*}\,\underline{f}$
3. Construct $\mathbb{L}$, $\mathbb{K}$, $\mathbb{P}$, and $\mathbb{Q}$ based on $\underline{A} = \mathbb{C}\underline{u} + \underline{k}$
4. Compute $\xi = \mathbb{L}^{-1}\mathbb{K}\underline{g}$.
5. Compute $\underline{\zeta} = \mathbb{P}^{-1}\mathbb{Q}\xi$.
6. Set $\underline{\psi} = \mathbb{T}_{\underline{v}}\,\underline{\zeta}$.

It is clear now that the discrete solution process satisfies the gauge-covariance test proposed above. That is, given gauge fields $\underline{A}$ and $\widetilde{\underline{A}}$ and source vectors $\underline{f}$ and $\widetilde{\underline{f}}$ defined in (42) and (43), Algorithm 4 will return $\underline{\psi}$ and $\widetilde{\underline{\psi}}$ such that $\underline{\psi} = \mathbb{T}_{\underline{\theta}}\,\widetilde{\underline{\psi}}$. To see this, notice that $\underline{A}$ and $\widetilde{\underline{A}}$

differ only by a gradient. Thus, for both sets of data, $\mathbb{L}$, $\mathbb{K}$, $\mathbb{P}$, and $\mathbb{Q}$ are all constructed using the same gauge field. Then

$$\underline{\psi} \;=\; \mathbb{T}_{\underline{v}} \, \mathbb{P}^{-1} \mathbb{Q} \mathbb{L}^{-1} \mathbb{K} \mathbb{T}_{\underline{v}}^* \, \underline{f}.$$

Similarly,

$$\begin{aligned}
\underline{\widetilde{\psi}} &\;=\; \mathbb{T}_{\underline{v}-\underline{\theta}} \, \mathbb{P}^{-1} \mathbb{Q} \mathbb{L}^{-1} \mathbb{K} \mathbb{T}_{\underline{v}-\underline{\theta}}^* \, \mathbb{T}_{\underline{\theta}}^* \, \underline{f} \\
&\;=\; \mathbb{T}_{\underline{v}-\underline{\theta}} \, \mathbb{P}^{-1} \mathbb{Q} \mathbb{L}^{-1} \mathbb{K} \mathbb{T}_{\underline{v}}^* \, \underline{f} \\
&\;=\; \mathbb{T}_{\underline{\theta}}^* \, \underline{\psi}.
\end{aligned}$$

Thus, setting $\underline{\psi} = \mathbb{T}_{\underline{\theta}} \, \underline{\widetilde{\psi}}$ yields the desired result.

2.4. Chiral Symmetry

Another physical property that a theory of QED should retain in the discrete setting is *chiral symmetry*. This property is a *global* symmetry that says that, in the massless case, independent constant rotations of the right- and left-handed components of the fermion field do not change the physics of the model. A sufficient condition for retaining chiral symmetry in the discrete setting is that the discrete Dirac operator, in the massless case, has zero main diagonal blocks. For a more thorough discussion of this property, see [9], [10], [11].

It is easy to verify that the proposed method retains chiral symmetry once it is clear what the discrete Dirac operator is. In fact, $\mathbb{D}$ is precisely the operator that relates $\underline{\psi}$ to $\underline{f}$, that is,

$$\mathbb{D}\underline{\psi} \;=\; \underline{f}.$$

From Algorithm 4, it is clear that, for the proposed method,

$$\mathbb{D} = \mathbb{T}_{\underline{v}} \, \mathbb{K}^{-1}\mathbb{L}\mathbb{Q}^{-1}\mathbb{P} \, \mathbb{T}_{\underline{v}}^{*}. \tag{48}$$

Setting $m = 0$ in (32) and (35), some simple algebra then shows that $\mathbb{D}$ has zero matrices as its main diagonal blocks. For a more rigorous discussion of chiral symmetry in the context of least-squares discretizations, see [3].

2.5. Species Doubling

A pitfall of many simple discretizations of the Dirac equation is that they suffer from what is known in the physics community as *species doubling*. Essentially, this means that, for every low frequency eigenvector of the discrete operator, a corresponding high frequency eigenvector shares the same eigenvalue. In the mathematics community this phenomenon is known as *red-black instability* [12]. It occurs as a result of naively discretizing first-order differential operators using a central-type difference scheme. The proposed method avoids this problem essentially by forming the normal equations in the continuum prior to the discretization by finite elements. The resulting discrete operator that must be inverted, namely, $\mathbb{L}$, has a 9-point stencil similar to that resulting from a Ritz-Galerkin discretization of a constant coefficient Laplacian. It is well known that discrete operators of this type do not suffer from red-black instability, and so the proposed discretization does not suffer from species doubling. For a more in-depth discussion of the phenomenon of species doubling, see [9], [10], or [11]. For a discussion of species doubling specifically in the case of a least-squares discretization, see [3].

In the physics community, there is a famous *no-go* theorem, attributed to Nielsen and Ninomiya, which has been interpreted as saying that a discretization of the Dirac equation cannot satisfy hermiticity, locality, and chiral symmetry without suffering from species doubling [9]. On the surface it appears that the discretization proposed here must violate this no-go theorem. However, the discrete least-squares operator avoids this because it is not local.

Although the proposed solution methodology only requires the inversion of matrices $\mathbb{L}$ and $\mathbb{P}$, which are local, the *effective* Dirac operator given in (48) is not a sparse matrix, and therefore not local.

3. Numerical Experiments

In this section, we apply adaptive smoothed aggregation multigrid (αSA) to solve matrix equation (31), which appears in Step 4 of Algorithm 4 [13]. The resulting linear system clearly contains complex entries. To avoid working in complex arithmetic, we solve the equivalent real formulation (ERF) of (31):

$$
\begin{bmatrix} \mathbb{X} & -\mathbb{Y} \\ \mathbb{Y} & \mathbb{X} \end{bmatrix} \begin{bmatrix} \underline{x} \\ \underline{y} \end{bmatrix} = \begin{bmatrix} \underline{a} \\ \underline{b} \end{bmatrix}, \tag{49}
$$

where $\mathbb{X}, \mathbb{Y}$ are real-valued matrices satisfying $\mathbb{L} = \mathbb{X} + i\mathbb{Y}$, $\underline{\xi} = \underline{x} + i\underline{y}$, and $\mathbb{K}\underline{f} = \underline{a} + i\underline{b}$.

Note that the matrix $\mathbb{P}$ appearing in (41) and Step 5 of Algorithm 4 does not depend on the gauge field. It is simply a mass matrix with constant coefficients. Solutions to linear systems involving $\mathbb{P}$ can be approximated quickly and efficiently by a number of methods. The vast majority of the solution process is spent approximating solutions of linear systems involving $\mathbb{L}$. As such, we focus the remainder of this section on the solution of (31).

3.1. Results

Table I reports average convergence factors of αSA applied to the homogeneous version of (49) and accelerated by conjugate gradients (CG) for various values of the particle mass, m, and gauge field temperature, β. Note that the smaller β is the more disordered the gauge field is. In all reported experiments, averages were taken over 20 distinct gauge fields. The αSA preconditioner was based on a single V(2,2)-cycle with 4 prototype error components used to build the interpolation operator. The relaxation scheme used was Gauss-Seidel. The operator

complexity, σ, is the ratio of the total number of nonzero matrix entries in the multigrid hierarchy to the number of nonzero entries in the fine-grid matrix.

$\beta \backslash m$	.001	.01	.1
2	.22	.20	.12
3	.18	.18	.10
5	.15	.15	.14

$\beta \backslash m$	.001	.01	.1
2	.22	.22	.13
3	.19	.20	.18
5	.16	.15	.11

$\beta \backslash m$	.001	.01	.1
2	.22	.21	.12
3	.22	.22	.17
5	.18	.17	.12

Table I: Average convergence factors for αSA-PCG applied to (49) on 64×64 (top), 128×128 (middle), and 256×256 (bottom) lattices with varying choices of mass parameter, m, and temperature, β. For each grid size, operator complexity, σ, was approximately 1.4.

In Table I, all tests have operator complexities of approximately 1.40. The method performs better for the largest mass tested and slightly worse for the two smaller masses. However, since performances remains fairly static between $m = .01$ and $m = .001$, it appears that critical slowing down has been eliminated. The value of β seems to affect the performance of the solver. As the value of β increases, the matrix becomes easier to invert. This is not surprising, since a larger β implies less disorder in the background gauge field. Finally, the solver appears to be scalable with respect to the lattice size.

4. Conclusions

We described a discretization of a modified version of the simplified model of QED based on least-squares finite elements. The modified continuum equations are obtained by applying a transformation that effectively removes the gauge field from the differential operators.

Discretizing the new system using least-squares finite elements results in a block-diagonal discrete operator with diffusion-like diagonal blocks. We presented a discrete algorithm that retains gauge covariance of the solution process and avoids species doubling. Finally, we applied adaptive smoothed aggregation multigrid to the resulting linear system. The numerical experiments demonstrate that the resulting system of linear equations can be approximately solved quickly and efficiently by an adaptive multilevel solver with convergence rates independent of grid size and mass of the particle.

ACKNOWLEDGEMENTS

REFERENCES

1. Brannick J, Brezina M, Keyes D, Livne O, Livshits I, MacLachlan S, Manteuffel T, McCormick S, Ruge J, Zikatanov L. Adaptive Smoothed Aggregation in Lattice QCD. *Lecture Notes in Computational Science and Engineering* 2007; **55**:507.

2. Brannick J, Brower R, Clark M, Osborn J, Rebbi C. Adaptive Multigrid Algorithm for Lattice QCD. *Physical Review Letters* 2008; **100**(4):41 601.

3. J Brannick, C Ketelsen, T Manteuffel, S McCormick. Least-squares finite element methods for quantum electrodynamics. *SIAM J. Sci. Comp.* 2009; Accepted.

4. Griffiths D. *Introduction to Elementary Particles*. Wiley-VCH, 2004.

5. Berndt M, Manteuffel T, McCormick S. Analysis of first-order system least squares (FOSLS) for elliptic problems with discontinuous coefficients: Part I. *SIAM J. Numer. Anal.* 2005; **43**:386.

6. Peskin M, Schroeder D. *An Introduction to Quantum Field Theory*. Addison-Wesley, 1995.

7. Cai Z, Lazarov R, Manteuffel T, McCormick S. First-order system least squares for second-order partial differential equations: Part I. *SIAM J. Numer. Anal.* 1994; **31**:1785.

8. Cai Z, Manteuffel T, McCormick S. First-order system least squares for second-order partial differential equations: Part II. *SIAM J. Numer. Anal.* 1997; **34**:425.

9. Nielsen H, Ninomiya M. Absense of neutrinos on a lattice: (I). Proof by homotopy theory. *Nucl. Phys. B* 1991; **185**:20.

10. Creutz M. *Quarks, Gluons and Lattices*. Cambridge University Press, 1983.

11. DeGrand T, DeTar C. *Lattice Methods for Quantum Chromodynamics*. World Scientific, 2006.

12. Wesseling P. *Principles of Computational Fluid Dynamics*. Springer, 2001.

13. Brezina M, Falgout R, MacLachlan S, Manteuffel T, McCormick S, Ruge J. Adaptive Smoothed Aggregation (alphaSA) Multigrid. *SIAM REVIEW* 2005; **47**(2):317.